Supplemental Data. Honsbein et al. (2009). A tripartite SNARE-K+ channel complex mediates in channel-dependent K+ nutrition in *Arabidopsis*.

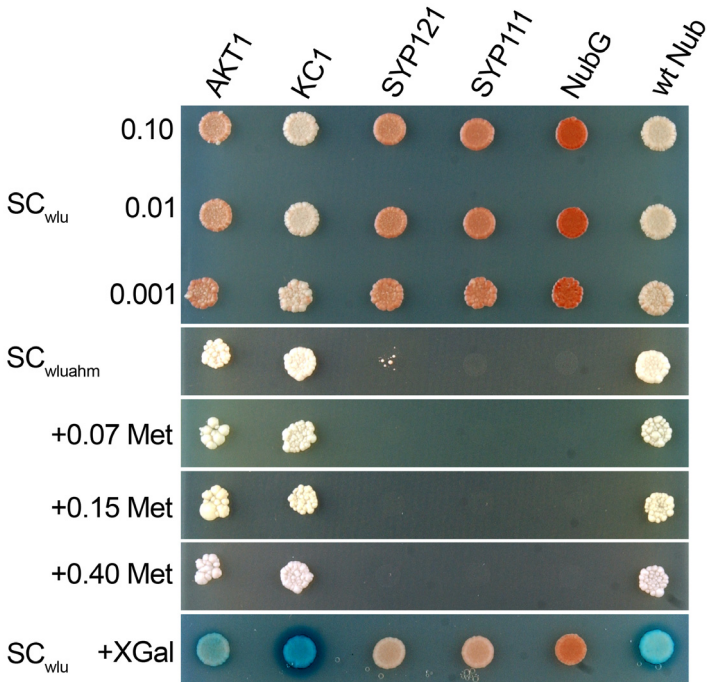

Fig. S1. AKT1 interacts with itself and the KC1 K^+ channel subunit, but not with the SNAREs SYP121 and SYP111 of *Arabidopsis*. Yeast mating-based split-ubiquitin assay for interaction with AKT1-Cub. Yeast diploid crosses with Nub-X constructs of AKT1, KC1, SYP121, SYP111, and controls (*negative*, NubG; *positive*, wild-type Nub) spotted (*left to right*) on SC medium without tryptophan, leucine and uracil (SC_{wlu}) to verify crossing and test for adenine synthesis (white colonies, top panel). SC without tryptophan, leucine, uracil, adenine, histidine and methionine (SC_{wluahm}) used to verify adenine- and histidine-independent growth (second panel), and the addition of 0.07, 0.15 and 0.40 mM methionine (next three panels) used to verify interaction at lower AKT1-Cub expression levels. SC medium without tryptophan, leucine and uracil (SC_{wlu}, last panel) used with an overlay of XGal-containing agarose to assay β-galactosidase activity (Obrdlik et al. 2004). Serial dilutions 0.1, 0.01 and 0.001 of diploid cultures as indicated for spots on SC_{wlu}. Otherwise only 0.1 dilutions shown. Note AKT1 interaction with KC1 and itself, and the absence of interaction with either SNARE.

Fig. S2. Fluorescence recovery after photobleaching (FRAP) analysis in a root hair expressing BiFC fusion constructs of SYP121 and KC1 with the N- and C-terminal halves of YFP (nYFP, cYFP), respectively.

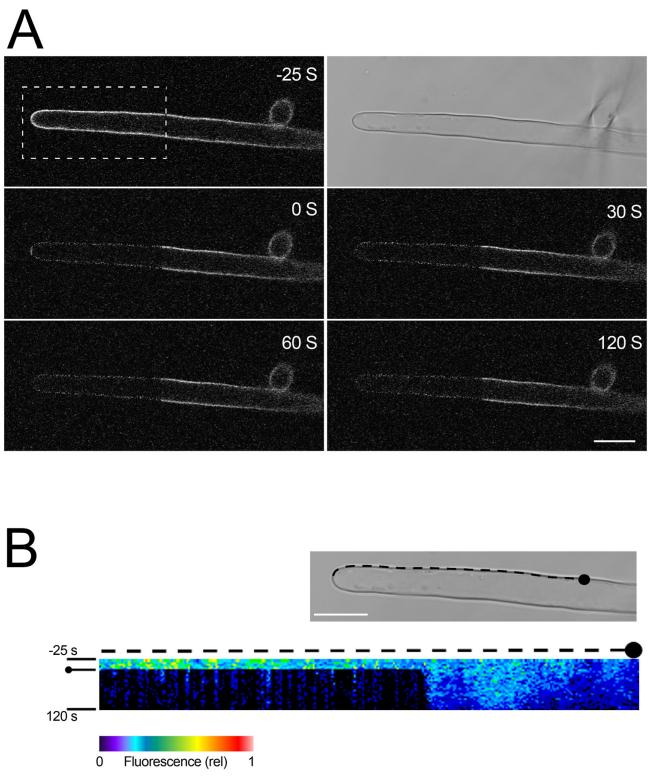

(A) Brightfield and fluorescence image taken before (-25 s, *above*) and at times after photobleaching (end of photobleach, relative t=0) the distal end of the root hair (photobleach area indicated in the first frame). Note the absence of an appreciable BiFC signal associated with trans-vacuolar cytoplasmic strands near the tip. Scale, 10 µm. Full time-lapse series will be found in Movie M1.

(B) Kymographic linescan analysis of relative fluorescence (color-coded scale as indicated) taken along line indicated in the brightfield thumbnail (*right*, white dotted line and orientation lollypop, corresponding line and lollypop above kymograph) shows the loss of signal in the distal half of the linescan after photobleaching and its lack of recovery, even adjacent the photobleach boundary. Scale bar: 10 µm.

Fig. S3. SYP121 expression alters channel gating of the AKT1-KC1 K^+ current in Sf9 insect cells.

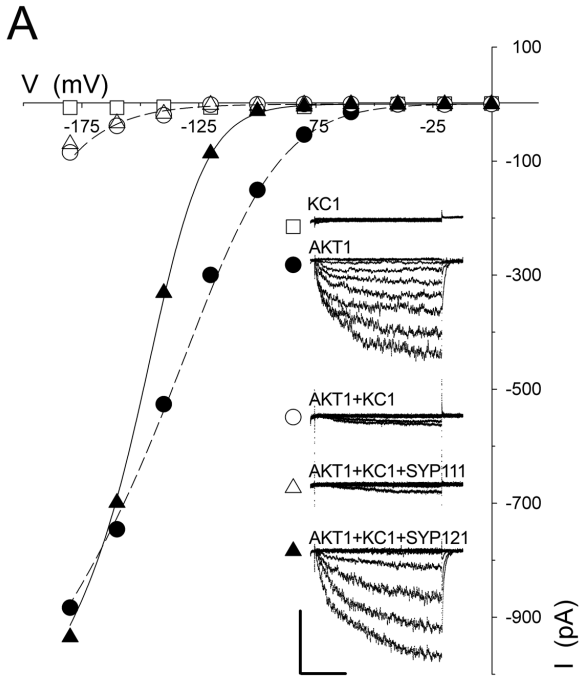

(A) Current-voltage curves and whole-cell currents (*insets*) recorded under voltage clamp in 100 mM K^+ from Sf9 cells expressing AKT1 alone (●), AKT1 with KC1 (○), AKT1 with KC1 and SYP121 (▲), and AKT1 with KC1 and SYP111 (Δ), and with KC1 alone (❑) as indicated. Expression verified by Western blot analysis (not shown). Clamp cycles: holding voltage, 0 mV; voltage steps (8), -20 mV to -180 mV. Scale: 500 pA and 500 ms. Currents from non-transfected cells, and cells expressing SYP111 or with SYP121 only gave results quantitatively similar to those KC1 (not shown). Currents from oocytes injected with AKT1 and SYP121 showed characteristics equivalent to those for AKT1 alone (not shown). Curves are the result of joint, non-linear least-squares fitting to a Boltzmann function with common g_{max} and δ allowed to vary between curves with and without SYP121. Parameter values: g_{max}, 5.44±0.04 nS; δ, -1.15±0.03 (-SYP121), -2.21±0.07 (+SYP121); $V_{1/2}$, -104±1 mV (AKT1), -218±3 mV (AKT1+KC1), -138±4 mV (AKT1+KC1+SYP121), -215±3 mV (AKT1+KC1+SYP111). Values for δ ±SYP121 differ significantly at P<0.01 (see text and Fig. 3).

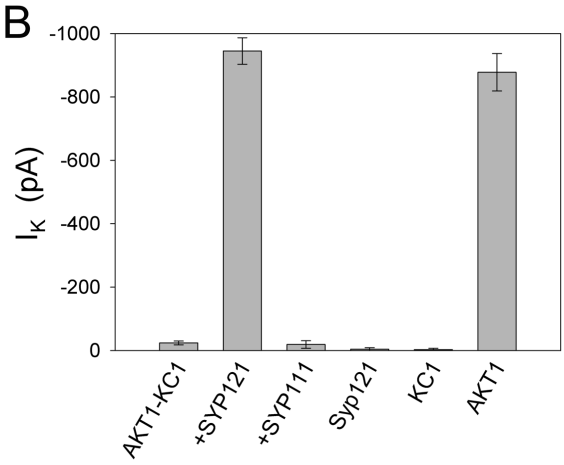

(B) Summary of K^+ current amplitudes recorded from Sf9 insect cells transfected with AKT1 alone, in combination with KC1, SYP111 and SYP121, and from Sf9 cells transfected with SYP121 and with KC1 alone. Data are means ±SE obtained at -180 mV from >5 independent experiments in each case (* differs significantly from AKT1+KC1 at P<0.01).

Fig. S4. *syp121* and *kc1* mutants of *Arabidopsis* show reduced growth and K^+ accumulation at low external [K^+] in the presence of NH_4^+. *Arabidopsis* seedlings germinated and grown in modified MS with 0.01 mM, 0.1 mM and 1.0 mM K^+, with and without NH_4^+.

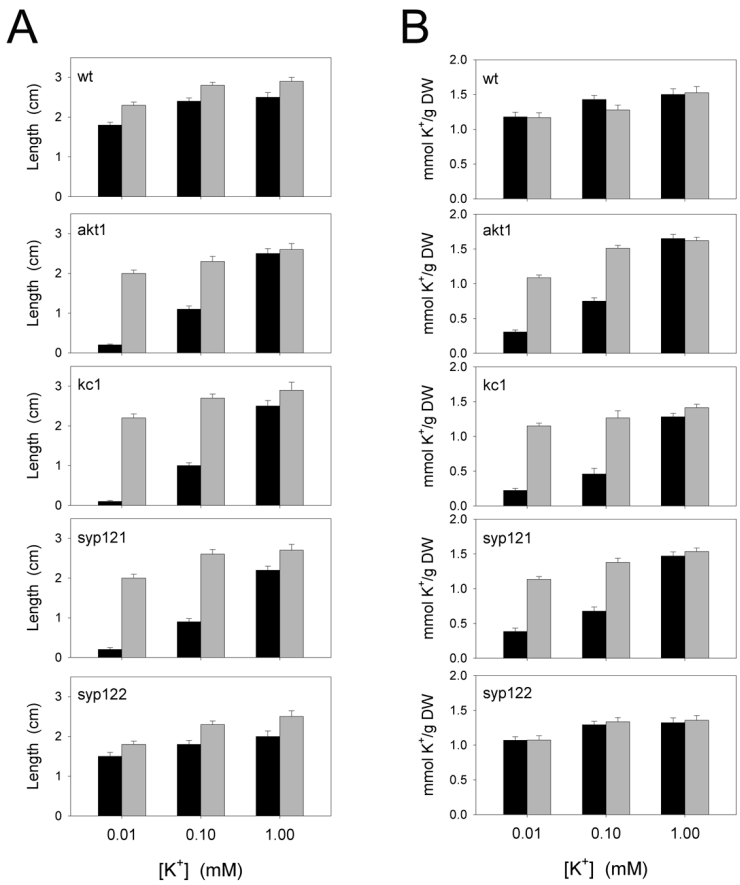

(A,B) Data summaries of root length (A) and total seedling K^+ contents normalized to dry weight (B) as means ±SE from three independent experiments (>80 seedlings per line for each growth condition) corresponding to the images in Fig.3.

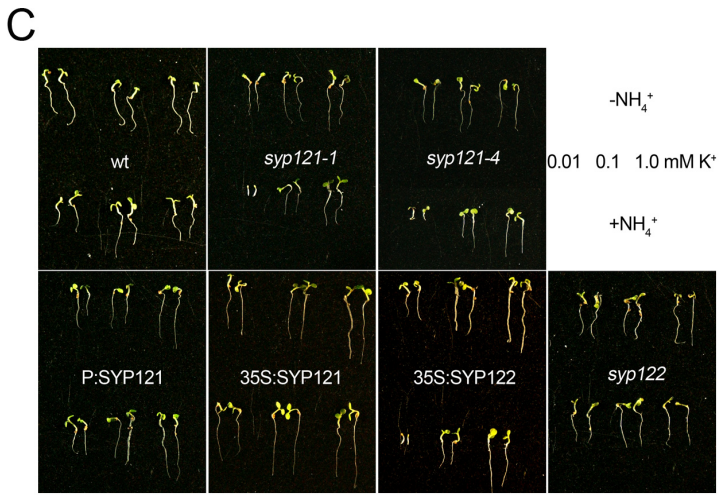

(C) Wild-type, *syp121* and *syp122* mutant alleles of *Arabidopsis* (Zhang et al. 2007) as indicated, and the *syp121-1* mutant complemented with Psyp121:SYP121-YFP (P:SYP121), 35S:SYP121-CFP (35S:SYP121) and 35S:SYP122-CFP (35S:SYP122 (Pajonk et al. 2008) germinated and grown for 7 d. Reference to growth conditions indicated in frame (*top right*). Scale bar, 1 cm.

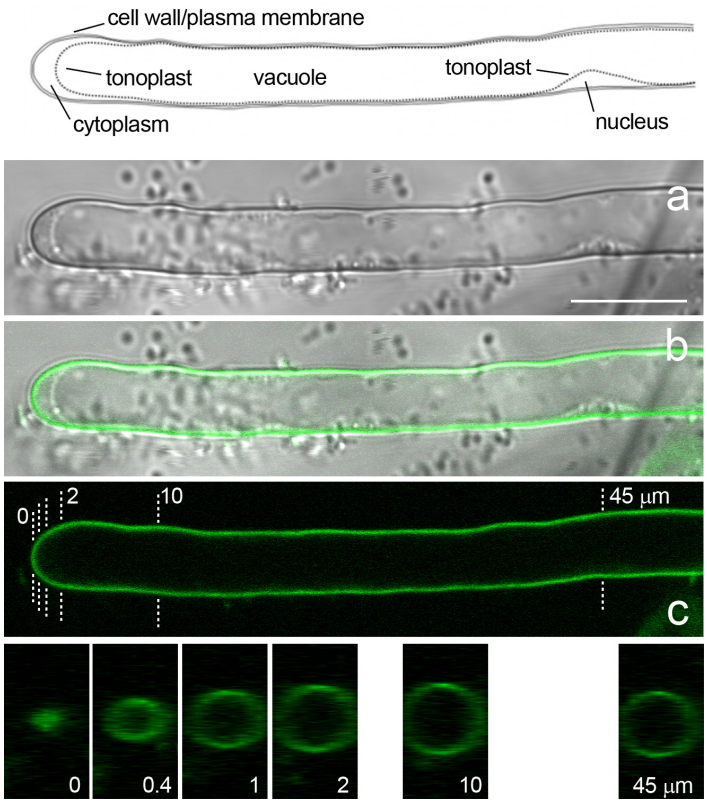

Fig. S5. The *syp121* mutation does not affect AKT1 K^+ channel expression at the root epidermal plasma membrane. Longitudinal section (*above*, brightfield, composite, GFP fluorescence) and three-dimensional transect analysis (*below*) of AKT1-GFP distribution in an *Arabidopsis syp121-1* mutant root hair. Transects taken at positions (in μm) from the apex as indicated by the dashed lines above. Note the peripheral distribution of the fluorescence and its virtual absence from the dense cytoplasm and tonoplast boundary behind the tip and around the nucleus (*top*, labelled schematic illustration drawn to scale for reference). Scale bar: 10 μm.

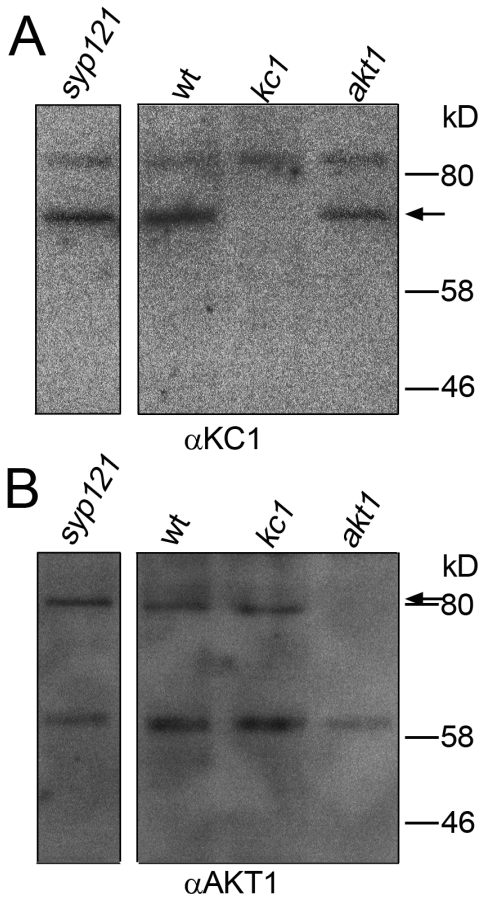

Fig. S6. Polyclonal antibodies generated against synthetic peptide antigens corresponding to unique amino-acid sequences H594-G608 of KC1 and C776-V789 of AKT1 recognize the corresponding K^+ channel proteins. Western blot analysis of total solubilized microsomal membranes (10 μg protein per lane) isolated from roots of wild-type, *kc1-2, akt1-1* and *syp121-1* mutant plants and probed with polyclonal antibodies to KC1 (A) and AKT1 (B) and visualised by phosphoimaging after secondary labelling with ^{125}I-labelled goat-antirabbit antibody (each blot edited to remove MW marker lanes). Both K^+ channels ran at apparent molecular weights below that predicted (arrows: KC1, 76.4 kD; AKT1, 97.0 kD) and were absent in membrane fractions from the corresponding null mutant. Additional non-specific bands appear at 80 kD with anti-KC1 and at 58 kD with anti-AKT1 antibody.

Supplemental Note

Are there K^+ currents in *kc1-f* mutant *Arabidopsis*?

One point of issue in interpreting the electrophysiological data relates to the absence of inward-rectifying K^+ current in our recordings from the *kc1* mutant root protoplasts (Fig. 4). By contrast, Reintanz, et al. (2002) reported an appreciable inward current from root hair protoplasts of the *Arabidopsis kc1-f* transposon mutant. This previous study does not include quantitative statistics that would enable direct comparison, but close inspection yields two, very straightforward explanations for the difference.

The first explanation relates to the nature of the currents. We note that the sample recordings illustrating the *kc1-f* mutant [see Fig. 4 of Reintanz, et al. (2002)] show a large fraction of the current comprised a non-gated, instantaneous component typical of a background current. This component is consistent neither with AKT1 current when heterologously expressed (Duby et al. 2008, Xu et al. 2006) nor with other inward-rectifier K^+ channels from plant roots (Buschmann et al. 2000, Dreyer et al. 2004, White and Lemtirichlieh 1995). Subtracting this component yields a residual, gated current at any one voltage corresponding to roughly 3-5 percent of the inward-rectifying K^+ current we observed in protoplasts from wild-type *Arabidopsis* (Fig. 4). We cannot rule out the presence of residual currents of this magnitude in our data Nonetheless, this analysis suggests that the predominant current observed by Reintanz, et al. in the mutant was not associated with the K^+ channels per se.

The second explanation relates to the different experimental conditions used in the two studies. We included millimolar concentrations of Na^+ in the bathing medium in order to match closely the alkali cation composition of the growth experiments. With one notable exception (below), Reintanz et al. included only K^+ salts. Normally plant K^+ channels are virtually insensitive to millimolar Na^+ in the bath and are almost equally permeable to K^+ and Rb^+ (Amtmann and Blatt 2007, Dreyer et al. 2004, Very and Sentenac 2003). However, Reintanz, et al. found that the *Arabidopsis kc1-f* mutant, unlike protoplasts from wild-type *Arabidopsis*, gave little or no inward current of any kind when 1 mM Rb^+ was included with K^+ in the bath. This altered sensitivity between the alkali cations is consistent with changes in access to and/or mobility through the channel and competitive block of the pore, and it implies similar changes in channel sensitivity to Na^+. As a second explanation then, it is possible that the mutant channel showed an enhanced sensitivity to block by Na^+ present in our bathing medium and, thus, did not exhibit a large, non-gated component similar to that of Reintanz, et al. Of course, if this were the case, then the same changes to the channel structure must have been overcome on SYP121 binding to enable K^+ permeation in the presence of Na^+ in our experiments.

Supplemental References

Amtmann, A. and Blatt, M.R. (2007) Regulation of ion transporters. In Plant Solute Transport, A.R.Yeo and T.Flowers, eds (Oxford: Blackwells), pp. 99-132.

Buschmann, P.H., Vaidyanathan, R., Gassmann, W., and Schroeder, J.I. (2000) Enhancement of Na^+ uptake currents, time-dependent inward- rectifying K^+ channel currents, and K^+ channel transcripts by K^+ starvation in wheat root cells. Plant Physiol. **122**:1387-1397.

Dreyer, I., MullerRober, B., and Kohler, B. (2004) Voltage-gated ion channels. In Membrane Transport in Plants, M.R.Blatt, ed (Oxford: Blackwell), pp. 150-192.

Duby, G., Hosy, E., Fizames, C., Alcon, C., Costa, A., Sentenac, H., and Thibaud, J.B. (2008) AtKC1, a conditionally targeted Shaker-type subunit, regulates the activity of plant K^+ channels. Plant J. **53**:115-123.

Reintanz, B., Szyroki, A., Ivashikina, N., Ache, P., Godde, M., Becker, D., Palme, K., and Hedrich, R. (2002) AtKC1, a silent *Arabidopsis* potassium channel alpha-subunit modulates root hair K^+ influx. Proc.Natl.Acad.Sci.USA **99**:4079-4084.

Very, A.A. and Sentenac, H. (2003) Molecular mechanisms and regulation of K^+ transport in higher plants. Annual Review of Plant Biology **54**:575-603.

White, P.J. and Lemtirichlieh, F. (1995) Potassium currents across the plasma membrane of protoplasts derived from rye roots - a patch clamp study. J.Exp.Bot. **46**:497-511.

Xu, J., Li, H.D., Chen, L.Q., Wang, Y., Liu, L.L., He, L., and Wu, W.H. (2006) A protein kinase, interacting with two calcineurin B-like proteins, regulates K^+ transporter AKT1 in *Arabidopsis*. Cell **125**:1347-1360.